



# Subsurface storage capacity influences climate–evapotranspiration interactions in three western United States catchments

E. S. Garcia<sup>1</sup> and C. L. Tague<sup>2</sup>

<sup>1</sup>Department of Atmospheric Sciences, University of Washington, Seattle, WA, USA

<sup>2</sup>Bren School of Environmental Science and Management, University of California, Santa Barbara, CA, USA

Correspondence to: E. S. Garcia (esgarcia@uw.edu)

Received: 2 July 2015 – Published in Hydrol. Earth Syst. Sci. Discuss.: 14 August 2015

Revised: 23 November 2015 – Accepted: 30 November 2015 – Published: 18 December 2015

**Abstract.** In the winter-wet, summer-dry forests of the western United States, total annual evapotranspiration (ET) varies with precipitation and temperature. Geologically mediated drainage and storage properties, however, may strongly influence these relationships between climate and ET. We use a physically based process model to evaluate how plant accessible water storage capacity (AWC) and rates of drainage influence model estimates of ET–climate relationships for three snow-dominated, mountainous catchments with differing precipitation regimes. Model estimates show that total annual precipitation is a primary control on inter-annual variation in ET across all catchments and that the timing of recharge is a second-order control. Low AWC, however, increases the sensitivity of annual ET to these climate drivers by 3 to 5 times in our two study basins with drier summers. ET–climate relationships in our Colorado basin receiving summer precipitation are more stable across subsurface drainage and storage characteristics. Climate driver–ET relationships are most sensitive to subsurface storage (AWC) and drainage parameters related to lateral redistribution in the relatively dry Sierra site that receives little summer precipitation. Our results demonstrate that uncertainty in geophysically mediated storage and drainage properties can strongly influence model estimates of watershed-scale ET responses to climate variation and climate change. This sensitivity to uncertainty in geophysical properties is particularly true for sites receiving little summer precipitation. A parallel interpretation of this parameter sensitivity is that spatial variation in storage and drainage properties are likely to lead to substantial within-watershed plot-scale differences in forest water use and drought stress.

## 1 Introduction

In high-elevation forested ecosystems in the western US, the majority of precipitation falls during the winter; there is often a disconnect between seasonal water availability and growing seasonal water demand. Consequently, forests in these regions are frequently water-limited, even when annual precipitation totals are high (Boisvenue and Running, 2006; Hanson and Weltzin, 2000). This disconnect between water inputs and energy demands also highlights the importance of storage of winter recharge by both snowpack and by soils. The importance of snowpack storage in these systems for hydrologic fluxes has received significant attention, particularly given their vulnerability to climate warming. Warmer temperatures are already shifting seasonal water availability in the western US through reductions in snowpack accumulation (Knowles et al., 2006) and earlier occurrence of peak snowpack (Mote et al., 2005) and shifts in streamflow timing (Stewart et al., 2005). Recently, field and modeling studies have shown that the years with greater snowpack accumulation can be a strong predictor of vegetation water use and productivity for sites in the California Sierra (Tague and Peng, 2013; Trujillo et al., 2012).

Less attention, however, has been paid to the role of subsurface storage and drainage that can influence whether or not winter precipitation or snowmelt is available for plant water use during the summer months. Previous studies have shown that plant access to stored water is a substantial contributor to summer evapotranspiration in semi-arid regions (Bales et al., 2011). Plant accessible storage includes both water stored in soil and in saprolite and bedrock layers that can be accessed by plant roots (McNamara et al., 2011). Like snowpack, the storage of water in the subsurface has the po-

tential to act as a water reservoir, storing winter precipitation for use later in the growing season (Geroy et al., 2011). The amount of water that can be stored varies substantially in space with topography, geologic properties, and antecedent moisture conditions (Famiglietti et al., 2008; McNamara et al., 2005). If the rate of snowmelt allows for subsurface moisture stores to be replenished later in the growing season, more of the winter precipitation is made available for plant water use. If storage capacity is too shallow to capture a significant amount of runoff or if the rate of rain or snowmelt inputs exceeds the rate of infiltration, then subsurface storage will not be physically able to extend water availability. While field studies in the western US have shown that shallow soils can limit how much snowmelt is available for ecological use during the summer (Kampf et al., 2014; Smith et al., 2011), these studies cannot fully characterize the relative impact of subsurface storage on ET given inter-annual and cross-site variation in climate drivers.

In this paper, we focus on the potential for plant accessible subsurface water storage to mediate the sensitivity of ET to inter-annual variation in climate drivers, precipitation and temperature. Understanding how ET varies with climate drivers is important, both from the perspective of how ET influences downstream water supply and water availability for forests and other vegetation (Grant et al., 2013). Western US forests show substantial vulnerability to drought, with declines in productivity and increases in mortality and disturbance in drought years (Allen et al., 2010; Hicke et al., 2012; Williams et al., 2013). Understanding these ecosystems' responses to primary climate drivers is of particular concern given recent warming trends (Sterl et al., 2008) and multi-year droughts (Cook et al., 2004; Dai et al., 2004) and that these changes in water and energy demands are expected to intensify (Ashfaq et al., 2013). Increased temperatures also affect plant phenology, leading to earlier spring onset of plant water use and productivity (Cayan et al., 2001), and thus can influence water requirements and water use. However, increases in early season water use, combined with higher atmospheric moisture demand, may lead to increased soil water deficit later in the season.

Forest evapotranspiration is also a substantial component of the water budget (Post and Jones, 2001) and thus any change in forest water use will potentially have significant impacts on downstream water use. Goulden et al. (2012), for example, use flux tower and remote sensing data to argue that warming may result in an increase of up to 60 % in vegetation water use at high elevations in the Upper Kings River watershed in California's southern Sierra watershed. We note however that these projected increases depend on how subsurface storage capacity interacts with snowpack at high elevations.

This paper's primary research objective is to quantify the interaction between subsurface storage characteristics and key climate-related metrics that influence forest water availability and use in snow-dominated environments receiving a range of summer precipitation. Heterogeneity in subsur-

**Table 1.** Explanatory variables.

Abbreviation	Definition
$P$	Total annual precipitation
$T_{AMJ}$	Average daily temperature for April, May, June
$R_{75}$	Day of water year by which 75 % of soil water recharge occurs
AWC	Available water capacity of soil (field capacity–wilting point)

face properties in soil, saprolite and bedrock layers makes the characterization of subsurface storage difficult at the watershed scale. Here we use a spatially distributed process-based model, the Regional Hydro-Ecologic Simulation System (RHESys), to quantify how uncertainty or spatial variation in subsurface storage properties might be expected to influence watershed response to these climate-related drivers. We apply RHESys in three case study watersheds of differing precipitation regimes to investigate how climate and subsurface storage combine to control inter-annual variation in ET.

## 2 Methods

We apply our model at a daily time step to three watersheds located in the western Oregon Cascades (OR-CAS), central Colorado Rocky Mountains (CO-ROC) and central California Sierras (CA-SIER). All three watersheds receive a substantial fraction of precipitation as snowfall, but vary in their precipitation and temperature regimes and amount of precipitation that falls as snow (Fig. 1). We compare a humid, seasonally dry watershed (OR-CAS) to two catchments that receive half as much precipitation annually. The more water-limited catchments differ in that CO-ROC receives a significant amount of its precipitation budget during the summer growing season. We use these case studies to estimate ET sensitivity to storage and drainage properties for several different precipitation and temperature regimes common in western US mountain watersheds. For each watershed, we quantify how subsurface storage and drainage properties interact with a combination of inter-annual variation in precipitation timing and magnitude, and shifts in snowpack storage. We first establish how inter-annual variation in three primary climate-related metrics (precipitation, average spring temperature, and timing of soil moisture recharge) influences annual ET with average subsurface storage properties. We then explore how these relationships change across physically plausible storage values.

### 2.1 RHESys model description

We use a physically based model (RHESys v.5.15) to calculate vertical water, energy, and carbon fluxes in our three

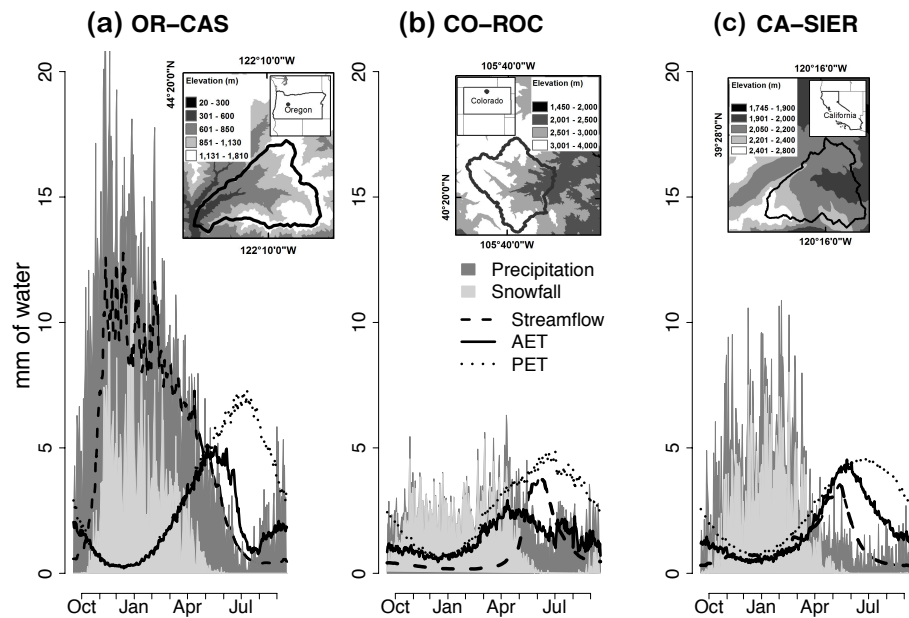


**Figure 1.** Locations and average daily water fluxes averaged from 1980 to 2000 for three case study watersheds located in (a) the western Oregon Cascades (OR-CAS), (b) Colorado Rockies (CO-ROC), and (c) California Sierra Nevada (CA-SIER).

**Table 2.** Basin topography, geology, vegetation and climate characteristics. Climate descriptions are averaged over the total available climate record (duration noted in table).

Watershed	CO-ROC	OR-CAS	CA-SIER
Location	Colorado	Oregon	California
US Geological Survey gage number	06733000	14161500	10343500
Geology	Holocene glacial till, rock; Precambrian gneiss, granite	Western Cascade basalt	Sierra granite, with Miocene andesite cap
Elevation range (m)	1470–4345	410–1630	1800–2650
Drainage area (km <sup>2</sup> )	350	64	26
Topographic wetness index – mean (SD)	7.0 (1.9)	6.6 (1.7)	7.9 (1.8)
Climate record	1980–2008	1958–2008	1960–2000
Mean annual precipitation (mm)	1000	2250	850
Annual precipitation as snow (%)	64	29	55
Precipitation received in growing season (%)	46	21	19
Min/max winter <i>T</i> (JFM) (oC)	–12.1/–0.02	–0.9/5.2	–9.5/3.7
Min/max spring <i>T</i> (AMJ) (oC)	–2.7/10.9	4.0/14.0	–2.5/13.8
P : PET	0.9	2.3	1.2
Vegetation	Subalpine fir, aspen, meadows, shrub	Douglas fir, western hemlock	Mixed conifer, Jeffrey and lodgepole pine
Mean basin LAI	3.5	9.0	4.1
Annual NPP range for calibration (gC m <sup>–2</sup> yr <sup>–1</sup> )	280–520	620–1100	450–800
Literature sources used to bound annual NPP range	Arthur and Fahey (1992) Bradford et al. (2008)	Grier and Logan (1977) Gholz (1982)	Hudiburg et al. (2009) Goulden et al. (2012)*

\* Values reported as gross primary productivity, converted to NPP using RHESSys-calculated values of respiration.

watersheds (Tague and Band, 2004). RHESSys is a spatially explicit model that partitions the landscape into units representative of the different hydro-ecological processes modeled (Band et al., 2000). RHESSys has been used to address diverse eco-hydrologic questions across many water-

sheds (Baron et al., 2000; Shields and Tague, 2012; Tague and Peng, 2013). Key model processes are described below and a full account is provided in Tague and Band (2004).

RHESSys requires data describing spatial landscape characteristics and climate forcing; a digital elevation model

(DEM) and geologic and vegetation maps are used to represent the topographic, geologic, carbon and nitrogen characteristics within a watershed. RHESSys accounts for variability of climate processes within the catchment using algorithms developed for extrapolation of climate processes from point station measurements over spatially variable terrain (Running and Nemani, 1987). Hydrologic processes modeled in RHESSys include interception, evapotranspiration, infiltration, vertical and lateral subsurface drainage, and snow accumulation and melt. The Penman–Monteith formula (Monteith, 1965) is used to calculate evaporation of canopy interception, snow sublimation, evaporation from subsurface and litter stores, and transpiration by leaves. A model of stomatal conductance allows transpiration to vary with soil water availability, vapor pressure deficit, atmospheric CO<sub>2</sub> concentration, and radiation and temperature (Jarvis, 1976). A radiation transfer scheme that accounts for canopy overstory and understory, as well as sunlit and shaded leaves, controls energy available for transpiration. RHESSys accounts for changes in vapor pressure deficit for fractions of days that rain occurs (wet versus dry periods). Plant canopy interception and ET are also a function of leaf area index (LAI) and gappiness of the canopy such that as LAI increases and gap size decreases, plant interception capacity and transpiration potential increases. RHESSys partitions rain to snow at a daily time step based on each patch's air temperature. Snowmelt is estimated using a combination of an energy budget approach for radiation-driven melt and a temperature index-based approach for latent heat-drive melt processes. Subsurface water availability varies as a function of infiltration and water loss through transpiration, evaporation and drainage. RHESSys also routes water laterally and thus patches can receive additional moisture inputs as either re-infiltration of surface flow or through shallow subsurface flow from upslope contributing areas. Lateral subsurface drainage routes subsurface and surface water between spatial units and it is a function of topography and soil and saprolite drainage characteristics. Deep groundwater stores are drained to the stream using a simple linear reservoir representation.

Carbon and nitrogen cycling in RHESSys was modified from BIOME-BGC (Thornton, 1998) to account for dynamic rooting depth, sunlit and shaded leaves, multiple canopy layers, variable carbon allocation strategies, and drought stress mortality. The Farquhar equation is used to calculate gross primary productivity (GPP) (Farquhar et al., 1980). Plant respiration costs include both growth and maintenance respiration and are influenced by temperature following Ryan (1991). Net primary productivity (NPP) is calculated by subtracting total respiration costs from GPP.

In our three study sites, RHESSys is driven with daily records of precipitation and maximum and minimum temperature. Each basin is calibrated for seven parameters that characterize subsurface storage and drainage properties. Drainage rates are controlled by saturated hydraulic conduc-

tivity ( $K$ ) and its decay with depth ( $m$ ). Air-entry pressure ( $\phi_{ae}$ ), pore size index ( $b$ ), and rooting depth ( $Z_r$ ) control subsurface water holding capacity (Brooks and Corey, 1964). In all basins, we assume that geologic properties allow for deeper groundwater stores that are inaccessible to vegetation (Table 2). Vegetation however can access more shallow groundwater flow. These deep groundwater stores are controlled by two parameters representing the percentage of water that passes to the store ( $gw_1$ ) and the rate of its release to streamflow ( $gw_2$ ). Calibration is conducted with a Monte Carlo based approach, the generalized likelihood uncertainty estimation (GLUE) method (Beven and Binley, 1992). Parameter sets (1000 in total) are generated by random sampling from uniform distributions of literature-constrained estimates for the individual parameters; all calibration parameter sets are physically viable representations of soils within each basin. In other words, though a single parameter set may not meet streamflow and annual NPP calibration metrics, that particular subsurface storage capacity may still exist within the basin.

Model validation and drainage/storage parameter calibration were performed using two measures: daily streamflow statistics and annual measures of NPP. Streamflow statistics were set such that good parameters resulted in daily flow magnitude errors of less than 15 %, Nash–Sutcliffe efficiencies (NSE, a measure of hydrograph shape) greater than 0.65, and logged NSE values greater than 0.7 (a test of peak and low flows) (Nash and Sutcliffe, 1970). We select all parameter sets from these acceptable values; the total number of parameters equals 87, 246, and 47 for CA-SIER, CO-ROC, and OR-CAS, respectively. Daily hydrologic fluxes are calculated over 15 years for each soil parameter set in order to account for variability due to parameters in establishing relationships with our climate-related indices, the results of which are presented in Figs. 2–4. We verify our annual ET estimates against limited field estimates published in literature for subwatersheds of CO-ROC and OR-CAS (Baron and Denning, 1992; Webb et al., 1978). The average of our model estimated annual ET matches these limited field-based measurements and also fall within the bounds of annual ET estimated through water balance by subtracting annual streamflow from our records of annual precipitation. We assess the performance of the carbon-cycling model by comparing with published forest field measurements of annual NPP (values reported in Table 2). In our fully coupled eco-hydrologic model, accurate estimates of NPP also suggest that ET estimates are reasonable. Finally we note that RHESSys estimates of ET and NPP have been evaluated in a number of previous studies by comparison with flux tower and tree ring data, and these studies confirm that RHESSys provides reasonable estimates of ET and its sensitivity to climate drivers (Vicente-Serrano et al., 2015; Zierl et al., 2007). We quantify the sensitivity of ET–climate relationships to geologic properties by varying subsurface storage parameters (Figs. 5–6).

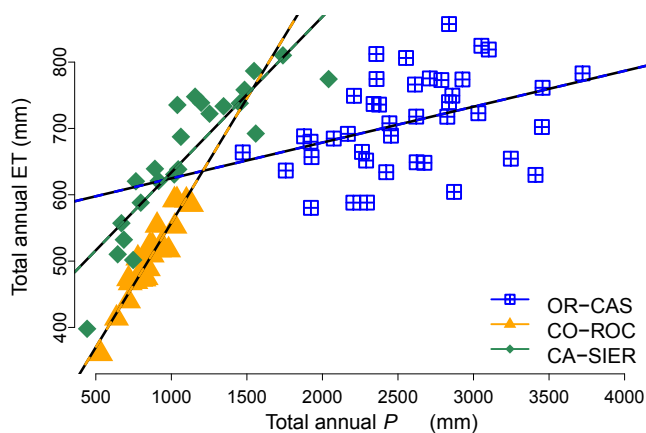


**Figure 2.** Total annual ET increases with total annual precipitation. Lines indicate statistically significant relationships ( $p$  value < 0.05).

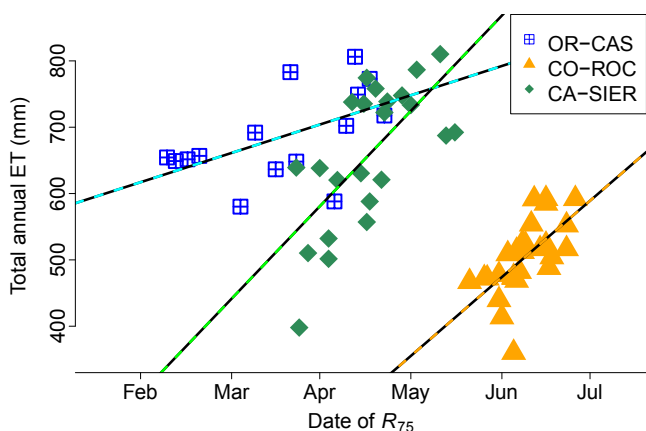


**Figure 3.** Later occurrence of soil moisture recharge ( $R_{75}$ ) is significantly correlated with increased annual ET in all study watersheds.

## 2.2 Study sites

These analyses are conducted in three western US mountain catchments: Big Thompson in Colorado’s Rocky Mountains (CO-ROC), Lookout Creek in Oregon’s Western Cascades (OR-CAS), and Sagehen Creek Experimental Forest in California’s northern Sierra Nevada (CA-SIER). Basin characteristics pertinent to modeling annual ET are listed in Table 2 and we highlight important similarities and differences here. All sites are located on steep, mountainous slopes and are dominated by forest cover. All basins have climates typical of the western US, on average receiving 54–81 % of their annual precipitation during the winter, 29–64 % of the annual  $P$  falls as snow, and they do not meet potential evaporative demand during the growing season (Fig. 1, Table 2). On average, OR-CAS is a much wetter basin and receives more than twice as much annual precipitation than CO-ROC and CA-SIER. Despite OR-CAS receiving more precipitation, a much lower fraction of that winter precipitation is received as

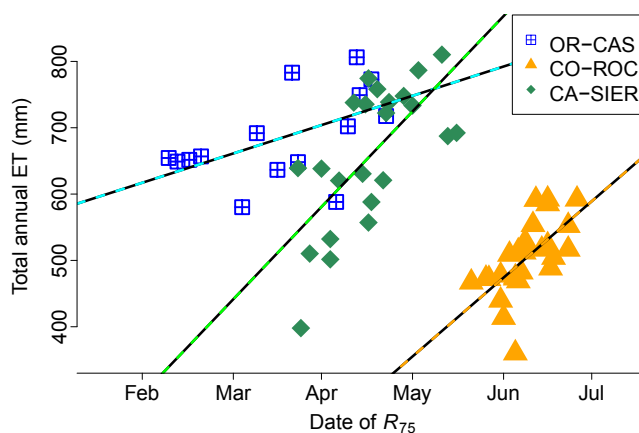


**Figure 4.** (a) Warmer spring temperatures are correlated with lower total annual ET in the two snow-dominated watersheds. (b) An earlier occurrence of soil moisture recharge is correlated with warmer temperatures in CO-ROC.

snow. On average, OR-CAS’s peak streamflow occurs in December, 4 to 5 months earlier than CO-ROC and CA-SIER (Fig. 1). The drier watersheds, CO-ROC and CA-SIER, receive more than half of their annual precipitation as snow (Table 2). CO-ROC also experiences a summer monsoonal season and on average receives 46 % of its annual precipitation from April to September. Landscape carbon (C) and nitrogen (N) stores in general vary with total annual  $P$  across basins. For example, OR-CAS receives the most precipitation and also supports stands of large, old-growth forests; its LAI is more than twice that of either CO-ROC or CA-SIER. As presented in the model description (Sect. 2.1), we use a stable, climatic optimum for vegetation biomass for all analyses in this paper. Garcia et al. (2013) and Tague and Peng (2013) provide detailed descriptions of the geology and climate data, model vegetation, and organic soil carbon store spin-up and calibration used for model implementations of OR-CAS and CA-SIER, respectively. We note that all precipitation and temperature data were derived from daily measurements made at climate stations located within the basins and extrapolated across the terrain using MT-CLM algorithms (Running and Nemani, 1987) and 30 m resolution DEMs. Though RHESSys has previously been used in CO-ROC (Baron et al., 2000), we have made significant updates in RHESSys since that time, so we re-implemented the model as described in the next section.

### 2.2.1 RHESSys model development for CO-ROC

In CO-ROC, landscape topographic characteristics including elevation, slope and aspect were derived from a digital elevation model (DEM) downloaded from the US Geologic Survey (USGS) National Elevation Dataset at 1/3 arcsec resolution (<http://datagateway.nrcs.usda.gov/>). A stream network was then derived to accumulate surface and subsurface flow

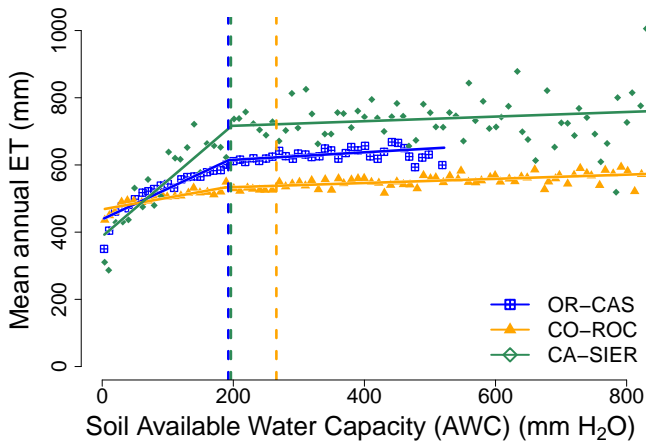


**Figure 5.** Each point represents the 15-year average annual ET from WY 1985 to 2000 for a physically viable mean basin soil available water capacity (AWC). Vertical lines represent the calculated break point in the nonlinear relationship between long-term ET and AWC for each basin.

at USGS gage no. 06733000. Sub-catchments were delineated using GRASS GIS’s watershed basin analysis program, *r.watershed*. Terrestrial data were aggregated such that the average size of the patch units, the smallest spatial units for calculation of vertical model processes, was 3600 m<sup>2</sup>. Soil classification data were downloaded from the Soil Survey Geographic database (SSURGO); <http://sdmdataaccess.nrcs.usda.gov/> and aggregated to four primary soil types: gravelly loam, sandy loam, loamy sandy, and rock (<http://datagateway.nrcs.usda.gov/>). Parameter values associated with these soil types are based on literature values (Dingman, 1994; Flock, 1978) and adjusted using model calibration, as described above. We note that these initial values are approximate and calibration permits storage values that reflect plant access to water stored in both organic soil layers and in sapprolite and rock. Vegetation land cover from the National Land Cover Database (NLCD) was aggregated to four primary vegetation types: subalpine conifer, aspen, shrubland, and meadow (Homer et al., 2007). Because a shift in precipitation patterns occurs at approximately 2700 m, we use daily records of precipitation,  $T_{max}$ , and  $T_{min}$  from two points within the watershed. RHESSys then interpolates data from these points based on MTN-CLM (Running and Nemani, 1987) to provide spatial estimates of temperature, precipitation and other meteorologic drivers for each patch. Climate data from 1980 to 2008 were downloaded from the DAYMET system for two locations – one at elevation 2460 m (latitude 40.35389, longitude –105.58361) and the second at 3448 m (latitude 40.33769, longitude –105.70315) (Thornton et al., 2012).

Plant C and N stores were initialized by converting remote-sensing-derived LAI to leaf, stem and woody carbon and nitrogen values using allometric equations appropriate to the vegetation type (<http://daac.ornl.gov/MODIS/>;

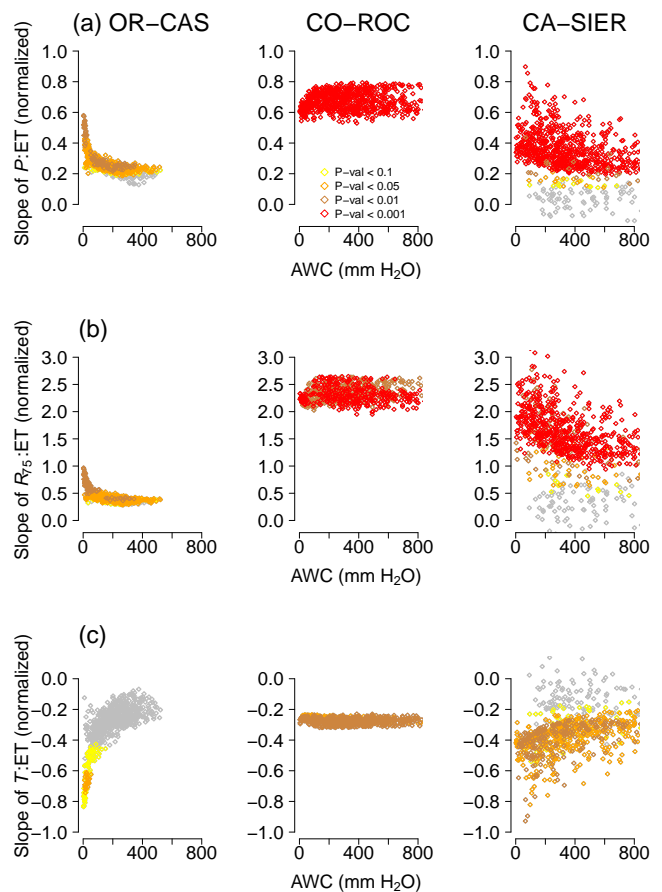


**Figure 6.** The impact of soil AWC on the slope of a linear regression model of annual ET as a function of climate predictors: (a) precipitation, (b)  $R_{75}$ , and (c)  $T_{AMJ}$ . The slope of the ET–climate predictor is plotted across a physically viable range of mean basin soil AWC for each climate predictor and for each study basin: OR-CAS (left column), CO-ROC (middle column), and CA-SIER (right column). The slopes are normalized to facilitate inter-basin comparison.

MOD15A2 Collection 5). In order to stabilize organic soil C and N stores relative to the LAI-derived plant C and N, we run the model repeatedly over the basin’s climate record until the change in stores stabilizes (Thornton and Rosenbloom, 2005). After stabilizing soil biogeochemical processes, we remove vegetation C and N stores and then dynamically “re-grow” them using daily allocation equations (Landsberg and Waring, 1997) for 160 years in order to stabilize plant and soil C and N stores with model climate drivers. For all three basins, an optimum maximum size for each vegetation type was determined using published, field-derived estimates of LAI and aboveground and total annual NPP.

### 2.3 Framework for primary controls on ET

In these seasonally water-limited basins, we use total annual precipitation ( $P$ ) as a metric of gross climatic water input. Annual precipitation  $P$  is summed over a water year (1 Oc-

tober to 30 September of the following calendar year) and summer season  $P$  is summed over July, August, and September. For all climate metrics we use spatially averaged watershed values. To assess the impact of timing of soil moisture recharge (as influenced either by year-to-year variation in precipitation timing, snowmelt or rain–snow partitioning) we calculate  $R_{75}$ , the day of water year by which 75 % of the total annual recharge has occurred. Recharge is defined as liquid water (e.g., rain throughfall or snowmelt) that reaches the soil surface. For this metric, we do not differentiate between water that, upon reaching the soil surface, becomes runoff, and water that infiltrates into the soil. We treat this variable as a temporal marker of potential water availability that denotes the timing within the water year that either rain throughfall or snowmelt may potentially infiltrate the soil. To examine energy inputs, we identify a season when temperature most strongly influences estimates of annual ET modeled using historic climate. We performed linear regressions between model estimate of total annual ET and 1- and 3-month averages of daily maximum ( $T_{\max}$ ), minimum ( $T_{\min}$ ) and average temperatures ( $T_{\text{avg}} = (T_{\max} + T_{\min})/2$ ) for all watersheds and for all months of the year. We test the correlation significance with a  $p$  value and set a significance threshold at 0.05; i.e., a  $p$  value greater than 0.05 is not significant. Our analysis found a 3-month average of daily  $T_{\text{avg}}$  in April, May and June ( $T_{\text{AMJ}}$ ) to have the greatest explanatory power as a temperature variable for estimating inter-annual variation in annual ET under historic climate variability across our three study watersheds (results not shown). We note that the  $p$  value for  $T_{\text{AMJ}}$  in CA-SIER was greater than 0.05, so it is not reported as a significant result. The growing season is assumed to extend from 1 May to 30 September in all watersheds. For all climate metrics we use spatially averaged watershed values.

We examine the role of storage through AWC. As noted above, plants access water organic soils as well as water stored in sapprolite and rock (Schwinning, 2010). We consider an aggregate storage and do not distinguish between these layers. AWC represents the water stored after gravity drainage (field capacity) that can be extracted by plant root suction (wilting point) and is thus still viable for plant water use (Dingman, 1994, p. 236). We calculate AWC as

$$\text{AWC} = (\theta_{\text{fc}} - \theta_{\text{wp}})Z_r. \tag{1}$$

Where  $\theta_{\text{fc}}$  represents the average field capacity per unit depth,  $\theta_{\text{wp}}$  the average characteristic wilting point also per unit depth, and AWC is scaled by vegetation rooting depth,  $Z_r$ , a model calibration parameter. The field capacity and wilting point are calculated, respectively, as

$$\theta_{\text{fc}} = \varphi(\phi_{\text{ae}} / 0.033)^b, \tag{2}$$

$$\theta_{\text{wp}} = \varphi(\phi_{\text{ae}} / \psi_v)^{1/b}, \tag{3}$$

Where  $\varphi$  is average subsurface porosity,  $\phi_{\text{ae}}$  represents the air-entry pressure (in meters),  $b$  is a pore size distribution

**Table 3.** Statistics for ET predictors based on linear regression models.

Watershed		CO-ROC	OR-CAS	CA-SIER
Precipitation ( $P$ )	$p$ value	<0.001	<0.05	<0.001
	$r^2$	0.9	0.1	0.75
	Slope	0.4	0.1	0.2
Timing ( $R_{75}$ )	$p$ value	<0.001	<0.01	<0.001
	$r^2$	0.2	0.2	0.4
	Slope	3.8	1.2	4.6
Temperature $T_{\text{AMJ}}$	$p$ value	<0.001	<0.05	>0.1
	$r^2$	0.4	0.1	–0.01
	Slope	–26.3	–25.7	15
Soil capacity (AWC)	$p$ value	0.001	0.001	0.001
	$r^2$	0.43	0.53	0.11
	Slope	0.1	0.2	0.1

index that describes the moisture-characteristic curve, and  $\psi_v$  describes the pressure at which the plants’ stomata close. Variables  $\phi_{\text{ae}}$  and  $b$  are also model calibration parameters.

Larger AWC indicates that more water can be held in the subsurface and potentially interacts with climate to extend plant water availability by capturing snowmelt, one of the primary sources of water for forest ET. Our results present each watershed’s average AWC; watersheds are represented by one (OR-CAS), two (CA-SIER), and five (CO-ROC) soil types and their characterizations are described in Table 2. All values of AWC calculated in the calibration represent physically feasible values for each watershed.

We use RHESSys to calculate total annual ET over the entire available climate record in each basin (28–50 years; Table 2) and use linear regression to quantify how much of the inter-annual variation in ET is related to each of the three climate metrics –  $P$ ,  $T_{\text{AMJ}}$ , and  $R_{75}$ . We set a limit of less than 0.05 for  $p$  values to determine significance. We then investigate how long-term mean ET and its relationship with these climate-related indicators are influenced by AWC.

To examine how subsurface storage capacity may influence long-term average ET, we calculate average annual ET over a 15-year period (1985–2000) for a range of 1000 AWC values and linearly regress the long-term averaged ET values against AWC. We then characterize the interacting influences of AWC and each climate driver. For the 1000 values of AWC, we calculate the slope of annual ET estimates to each climate predictor ( $P$ ,  $T_{\text{AMJ}}$ ,  $R_{75}$ ).

### 3 Results

#### 3.1 Annual $P$ vs. ET

In all watersheds higher  $P$  results in greater total annual ET (Fig. 2). This is a statistically significant relationship in all

watersheds (CO-ROC and CA-SIER, correlations and  $p$  values reported in Table 3) where the years of highest annual  $P$  are correlated with the years of greatest annual ET. Of the three basins, CO-ROC's annual ET shows the greatest sensitivity to  $P$ , having the steepest slope. Annual  $P$  is the strongest explanatory variable of annual ET in both CO-ROC ( $r^2 = 0.9$ ) and CA-SIER ( $r^2 = 0.75$ ) (Table 3). For CO-ROC, annual  $P$  has a greater influence (steeper slope) in the drier years when  $P$  is less than 1000 mm (Fig. 2). OR-CAS has the least significant relationship between  $P$  and ET on an annual scale. OR-CAS is a relatively wet basin and on average receives more than twice the amount of winter (January–March) precipitation than CA-SIER or CO-ROC receives. High annual  $P$  in OR-CAS in most years likely diminishes the sensitivity of ET to the magnitude of  $P$ .

### 3.2 Timing of recharge vs. ET

For all three catchments, later  $R_{75}$  has a significant positive correlation with ET (Fig. 3). In OR-CAS and CA-SIER,  $R_{75}$  occurs between February and May. There is more scatter in the predictive power of  $R_{75}$  for annual ET when  $R_{75}$  is earlier in the water year. The earliest  $R_{75}$  is in OR-CAS, where a greater fraction of winter precipitation falls as rain. CA-SIER and CO-ROC are more sensitive to the timing of recharge than OR-CAS. Summer monsoonal pulses in CO-ROC push  $R_{75}$  to later in the water year as compared to OR-CAS or CA-SIER. The explanatory power of  $R_{75}$  for ET is greatest in CA-SIER where greater accumulation of snowpack and warmer spring temperatures can interact to increase forest water use earlier in the growing season.

### 3.3 Spring temperature vs. ET

Warmer spring temperature ( $T_{AMJ}$ ) in all basins generally reduces annual ET (Fig. 4a) and is significantly correlated with lower ET in CO-ROC and OR-CAS. CA-SIER does not show a significant relationship between  $T_{AMJ}$  and ET. In CO-ROC and OR-CAS, increasing  $T_{AMJ}$  leads to a reduction in water availability and a decline in later season ET. The relationship between spring air temperature and snowmelt timing is demonstrated by significant correlations between  $T_{AMJ}$  and  $R_{75}$  for CO-ROC (Fig. 4b). The colder temperatures and more persistent snowpack in the CO-ROC basin are more sensitive, relative to OR-CAS, in ET response to earlier snowmelt due to temperature increases.

### 3.4 AWC vs. ET

Increased AWC increases the long-term average ET in all basins. Figure 5 shows a nonlinear relationship between long-term mean ET and AWC, suggesting that the effect of increasing storage diminishes for higher AWC values. Each basin reaches an approximate storage capacity above which a further increase in storage (AWC) is less important and climate (i.e.,  $P$  and energy) variables limit ET. Following

Muggeo (2003), for each basin, we calculate that breakpoint value of AWC where ET is less sensitive to AWC. We find that the threshold value of AWC varies across basins and is substantially higher in CO-ROC (265 mm) as compared to CA-SIER (195 mm) and OR-CAS (190 mm) (Fig. 5). Regression of AWC against annual ET shows that a significant relationship exists in OR-CAS and CO-ROC (Table 3).

The effect of varying lateral redistribution or lateral drainage parameters can be seen in the range of slopes for a given AWC (e.g., the scatter in the slope–AWC relationship). All three watersheds show some sensitivity of climate–ET relationships to lateral redistribution parameters for a given AWC. CA-SIER shows the greatest sensitivity, followed by OR-CAS and CO-ROC. The greater sensitivity of CA-SIER to lateral drainage parameters may reflect the strong contribution of snowmelt recharge in its drier and winter precipitation dominated climate. The topography of CA-SIER is also distinctive and includes many swale-like features that concentrate drainage from upslope areas. We calculate the topographic wetness index (TWI) using a 30 m resolution DEM for each watershed (Moore et al., 1991) (Table 2). The TWI reflects the propensity of a location to develop saturated conditions under the assumption that topography controls water flow. Higher TWI values represent flatter, converging terrain and lower values reflect steep topography. The mean TWI for CA-SIER is greater than and significantly different from (Welch's  $t$  test) the mean TWI for CO-ROC and OR-CAS. Particularly for CA-SIER, changing storage parameters associated with drainage rates can alter the timing of flow into areas that concentrate flow and subsequently alter their ET rates.

### 3.5 Sensitivity of ET to climate drivers with AWC

We analyze the sensitivity of ET relationships with climate drivers to subsurface storage properties by plotting the slope of linear regressions between ET and  $P$ ,  $R_{75}$ , and  $T_{AMJ}$ , across all storage parameter sets in Fig. 6. We note that the slope of the relationships between climate drivers and ET has been normalized by the watersheds' mean AWC in these plots to facilitate cross-site comparison.

#### 3.5.1 Sensitivity to $P$ with AWC

Of the climate drivers explored, ET relationships with annual precipitation  $P$  have the greatest robustness across subsurface storage parameter sets, as suggested by the number of sets that show a statistically significant relationship between annual  $P$  and annual ET (Fig. 6a). As expected, slopes are positive between  $P$  and ET across all basins. Only the drier basins CO-ROC and CA-SIER have  $p$  values less than 0.001, highlighting the strength of  $P$  as a climatic driver in these drier basins, as discussed above. The response in slope sensitivity across AWC is similar in OR-CAS and CA-SIER, where ET's sensitivity to  $P$  is highest at low AWC and de-

creases with increased AWC. OR-CAS has a much smaller range in sensitivities (slope varies from 0.2 to 0.6) compared to CA-SIER (slope varies from 0.0 to 0.8). Thus in CA-SIER for low values of AWC, year-to-year variation in  $P$  becomes a greater control on year-to-year variation in ET. For both OR-CAS and CA-SIER, increasing AWC becomes less important at higher values of AWC. Higher scatter in slope of annual  $P$  versus ET relationship for CA-SIER also reflects the greater sensitivity of ET to subsurface parameters that influence lateral drainage as discussed above (Sect. 3.4).

The variation of ET response to  $P$  across AWC in CO-ROC is noteworthy for two reasons. First, CO-ROC has the highest slope values (0.6–0.8), which again reflects the consistency of annual  $P$  as a control on inter-annual variation in ET in this basin. Second, unlike OR-CAS and CA-SIER, increasing AWC does not substantially reduce that sensitivity (i.e., slope) to  $P$ . Though CO-ROC's sensitivity to  $P$  does not change with AWC, the scatter in slopes (0.6–0.8) suggests that lateral drainage has a strong effect on this climate–ET relationship. We note that CO-ROC has a seasonal precipitation regime where a significant fraction of its annual precipitation is received later in the growing season as summer monsoonal pulses. When precipitation occurs during the growing season, the water available for ET is less likely to be limited by storage capacity. Instead ET is limited by the amount or intensity of precipitation. Water that does recharge the system is used relatively quickly, making variation in storage (or AWC) less important as a control on how much  $P$  can be used in CO-ROC.

### 3.5.2 Sensitivity to $R_{75}$ with AWC

After precipitation, the timing of recharge ( $R_{75}$ ) most significantly correlates with increased ET across all AWC and all basins (Fig. 6b). There are several similarities in the response of ET's sensitivity to  $R_{75}$  across AWC when compared to sensitivity to  $P$  (Fig. 6a). For example, the dry basins CO-ROC and CA-SIER have the highest degree of sensitivity (significant slopes  $>1.0$ ) as compared to OR-CAS (slopes  $<1.0$ ) and CA-SIER has the greatest variability in its sensitivity to AWC, with slopes ranging from 1.0 to 3.0 across variation in storage parameters. CO-ROC once again has the least variability in the ET versus  $R_{75}$  relationship, with consistently high (2.0–2.5) slopes unaffected by AWC.

### 3.5.3 Sensitivity to $T_{AMJ}$ with AWC

Finally,  $T_{AMJ}$  has the fewest subsurface storage/drainage parameter sets with significant correlation with ET. None of the linear regressions of ET on  $T_{AMJ}$  have statistical significance less than 0.001 (Fig. 6c). The slopes are always negative because earlier occurrence of snowmelt results in less ET. For all basins, the sensitivity of ET to  $T_{AMJ}$  is greatest at the lowest values of AWC, though CO-ROC once again demonstrates the least variability in slopes across the entire range

of AWC (−0.2–−0.3). At OR-CAS,  $T_{AMJ}$  is only significant for the lower AWC values. We suggest this is in part due to the small fraction of  $P$  that falls as snow. Because  $T_{AMJ}$ 's largest effect is through timing of snowmelt (Fig. 4), AWC interacts with  $T_{AMJ}$  to modulate the melt response. With relatively less snowmelt in OR-CAS, only the systems with the smallest capacities will have a significant negative interaction effect with AWC.

## 4 Discussion

Our model estimates show differences in the response of ET to climate-related drivers across the three watersheds, primarily due to differences in their precipitation regimes. Spatial heterogeneity in soil and geology, both within and between watersheds, substantially alters these relationships. Our model-based study provides a simplified representation of these interactions, ignoring many additional complexities. In particular, we assume no adaptation of the ecosystem structure and composition that would influence productivity, evapotranspiration and their relationship with climate (Loudermilk et al., 2013). Future work will investigate these coupled carbon cycling–hydrology interactions. In this study we focus on the energy and moisture drivers of ET and how subsurface properties influence their interaction.

The degree to which climate drivers affect ET varies with the magnitude and seasonality of basin precipitation. Total annual  $P$  is the first-order control of ET in the two drier watersheds, CO-ROC and CA-SIER. In OR-CAS, most of the inter-annual variation in precipitation is reflected in inter-annual variation in runoff rather than ET. In most years, subsurface storage is filled by this annual precipitation during the winter and spring, asynchronously to late growing season demands (Fig. 1). Our results extend findings by previous studies demonstrating that vegetation productivity and water use relate to the fraction of regional precipitation available to plants (Brooks et al., 2011; Thompson et al., 2011). The fraction of water available to plants tends to decrease with larger rainfall (given saturated soil stores, a greater proportion is lost) and with synchronicity between the timing of recharge and growing season water demands.

Our analysis highlights the timing of water availability ( $R_{75}$ ) as a key predictor of total annual ET; annual ET increases when recharge occurs later in the water year, during the growing season and period of highest water demand. Previous research has shown how delayed soil moisture recharge (Tague and Peng, 2013) and snowpack dynamics (Tague and Heyn, 2009; Trujillo et al., 2012) are able to increase ET in the Sierra Nevada. In these mountain basins, the sensitivity of ET to timing of recharge is related to the fraction of precipitation received as snow. The climate metrics related to snowmelt,  $R_{75}$  and  $T_{AMJ}$ , are important secondary controls of ET, especially in the colder, snow-dominated watersheds, CA-SIER and CO-ROC. We note that CA-SIER does

not show a significant relationship between  $T_{AMJ}$  and ET because the effect of temperature is strongly dependent on the amount of snowpack the basin receives in a year (Tague and Peng, 2013), which is more variable than the amount of snowpack received in CO-ROC or OR-CAS. In OR-CAS and CO-ROC, spring temperature  $T_{AMJ}$  is more strongly related to ET through its effect on snowmelt, and correlates negatively with ET. These results suggest that the dominant effect of warmer spring temperatures is earlier meltout of snowpack, which leads to more snowmelt lost as runoff and results in less net recharge. This greater loss of runoff occurs when storage capacity is exceeded. Later in the growing season, increased ET demands will have depleted subsurface stores and throughfall/snowmelt will enter the soil matrix and be available for plant water use. Previous work has shown seasonal increases in spring ET with warmer spring temperatures (Hamlet et al., 2007) that may be related to an earlier start to the vegetation growing season (Cayan et al., 2001) and an increase in vapor pressure deficits and water demand (Isaac and van Wijngaarden, 2012). Our work suggests that though early season ET may increase with warming temperatures, warmer spring temperatures may in some cases decrease total annual ET by melting the snowpack stores earlier in the water year and reducing soil moisture recharge later in the spring when energy demand is high.

The range of sensitivities of ET to climate in this study is a direct function of climatic and physical characteristics of the catchments presented in this study. For example, OR-CAS receives twice as much precipitation and spans a much lower elevation range than either CA-SIER or CO-ROC (Table 2). Because OR-CAS is considerably wetter, its sensitivity of ET to the magnitude of annual  $P$  is lessened considerably. OR-CAS' lower elevations, and related mean winter temperatures, also result in smaller average snowpacks reducing the strength of spring temperature as an explanatory variable for ET. Differences between CA-SIER and CO-ROC largely reflect seasonal distribution of precipitation, and reflect the importance of summer precipitation in CO-ROC. While climate is the dominant factor, topographic differences are also important. As discussed above, topographically driven flowpath convergence in CA-SIER tends to increase sensitivity of ET to parameters that influence lateral drainage. This effect is less evident in the other two watersheds.

Over a range of physically realistic storage characteristics, long-term averages of ET increase with greater storage (AWC) in all basins. Our analysis found the greatest sensitivity of long-term average annual ET to variation in AWC in OR-CAS (Table 3). In CO-ROC, ET ranges from 380 to 600 mm across annual  $P$  variation, and across all calibrated subsurface parameters long-term average ET ranges from 450 to 600 mm. This variation in CO-ROC's ET associated with subsurface storage characteristics is on the same order of magnitude as inter-annual variation in ET with  $P$ . Similarly, in CA-SIER, ET ranges from 400 to 800 mm across the  $P$  record and across all storage parameters, and ranges from

700 to 1000 mm long-term. There is a nonlinear relationship between ET and AWC in each basin. We suggest that below a threshold point in each basin (195–265 mm of AWC), long-term average ET is more sensitive to AWC, and above these threshold values, the effect of climate on ET is greater than an increase in subsurface storage.

The sensitivity of ET to year-to-year variability of climate drivers is also influenced by AWC. The sensitivity of ET estimates to climate drivers varies by 2 to 5 magnitudes in CA-SIER and OR-CAS across the range of plausible storage parameters. These basins receive the smallest fraction of annual  $P$  in the summer, and their annual ET estimates are most sensitive to  $P$ ,  $R_{75}$ , and  $T_{AMJ}$  at low water capacity (AWC). CO-ROC has a high sensitivity to climate drivers, but this sensitivity does not change with AWC. We suggest that a strong summer  $P$  signal in CO-ROC explains the negligible change in ET's sensitivity to climate drivers across values of AWC, similar to other studies that show that summer  $P$  can offset the dependence of ET on soil replenishment or winter snowpack (Hamlet et al., 2007; Litaor et al., 2008). The relative importance of AWC to regional climate differences is apparent if we consider that a similar sensitivity to  $P$  and  $T_{AMJ}$  can be achieved for all basins by varying AWC. For example, ET at the smallest AWC values in OR-CAS is similarly sensitive (slope of 0.6) to inter-annual variation in precipitation as CO-ROC (Fig. 6a).

The two more water-limited basins demonstrate similarly high sensitivities of ET to climate drivers, but differ in the response of their sensitivity to climate across AWCs. Despite CO-ROC and CA-SIER showing similarly strong sensitivities to climate, their response across AWC differs considerably. CA-SIER's sensitivity to climate drivers is highly variable across all AWC, but still demonstrates slightly higher sensitivity at lower AWC values. Its lack of summer precipitation, like OR-CAS, gives water storage a more significant role in mediating late summer water stress. With lower AWC values there is less potential for water storage and ET becomes more sensitive to climate drivers.

In addition to the sensitivity to AWC, our results show that lateral redistribution strongly influences the sensitivity of ET to climate drivers in the drier basins; in CA-SIER and CO-ROC there is considerable scatter in the slopes for  $P$  and  $R_{75}$  across a single AWC (e.g., for an AWC of 400 mm, the  $P$ :ET ranges from 0.6 to 0.8 and 0.2 to 0.7 for CO-ROC and CA-SIER, respectively, in Fig. 6). We note that this additional sensitivity of ET–climate relationships to drainage rates, even given similar AWC or storage conditions, emphasizes the role played by lateral connections. In other words, results suggest that for the two more water-limited sites, the timing of upslope contributions to downslope areas can mediate the sensitivity of watershed-scale vegetation water use.

Our results have general implications for model-based estimates of ET in this region. Because there is substantial heterogeneity in subsurface storage characteristics within each basin (Dahlgren et al., 1997; Denning et al., 1991; McGuire

et al., 2007), we might expect that the full range of AWCs can be observed when we look across individual forest stands within a basin. Thus, our estimates that show substantial changes in climate–ET relationships across subsurface parameters suggest that there may be substantial within-basin spatial heterogeneity in vegetation responses to climate variation and change. Even if model estimates are focused on basin aggregate responses such as streamflow, our results point to the importance of calibration data for defining subsurface storage and drainage properties. Estimates of subsurface parameters are often derived from readily available products such as STATSGO and SSURGO (Natural Resources Conservation Service) that provide relatively coarse-scale and imperfect information about hydrologic properties. Consequently, hydrologic models are typically calibrated to obtain estimates of storage and drainage parameters (Beven, 2011). Our results suggest that in areas where streamflow data are not available for calibration, watershed-scale estimates of ET responses to climate drivers may have substantial errors.

## 5 Conclusions

We demonstrate how subsurface storage and drainage properties (AWC and parameters that control lateral redistribution) interact with climate-related drivers to influence ET in three western US mountain watersheds with distinctive precipitation regimes. These watersheds reflect conditions found in many other western US snow-dominated systems, where summer water availability is influenced by the magnitude of precipitation, timing of soil moisture recharge and spring temperature and its effect on snowmelt. We found that, for our three watersheds, estimates of longer-term average (15-year) watershed-scale ET vary across a range of physically realistic storage/drainage parameters. For all watersheds, the range in long-term mean ET estimates across AWC estimates (e.g., mean ET at a high AWC versus mean ET at a low AWC) may be as large as inter-annual variation in ET, suggesting that the influence of AWC and drainage can be substantial.

Our results also point to the importance of lateral redistribution as a control on ET, particularly for CA-SIER. Only a few studies have emphasized the role of lateral redistribution in plot- to watershed-scale climate responses in the western US (Barnard et al., 2010; Tague and Peng, 2013). For the CA-SIER site, our model results suggest that there can also be interactions between AWC and hillslope to watershed-scale redistribution as controls on ET. Lateral redistribution was less important for the CO-ROC, where summer precipitation was a more important contributor to annual ET values and the least important for the wetter OR-CAS site. Results emphasize that the role of subsurface properties, including both storage and drainage, will be different for different climate regimes.

These results have important implications both for predicting ET in basins where data are not available for calibration and for understanding and predicting the spatial variability of ET within a basin. AWC also affects the sensitivity of annual ET to climate drivers, particularly in the two more seasonally water-limited basins. Although the three watersheds show different responses of annual ET to these climate drivers, there are values of AWC that would eliminate these cross-basin differences. These sensitivities highlight the need for improved information on spatial patterns of subsurface properties to contribute to the development of science-based information on forest vulnerabilities to climate change. Improved accounting for plant accessibility to moisture has improved model–data ET comparisons in previous modeling studies on regional and global scales (Hwang et al., 2009; Tang et al., 2013; Thompson et al., 2011). With expected decreases in fractional precipitation received as snow with climate change (Diffenbaugh et al., 2013; Knowles et al., 2006), we might expect soil storage to play a more important role in providing water for forests in the future. Improved understanding of how climate and subsurface storage/drainage combine to control ET can enhance our understanding of forest water stress related to increased mortality (van Mantgem et al., 2009). Western US forests show substantial vulnerability to drought, with declines in productivity and increases in mortality and disturbance in drought years (Allen et al., 2010; Hicke et al., 2012; Williams et al., 2013). Understanding these ecosystems' responses to primary climate drivers is of particular concern given recent warming trends (Sterl et al., 2008) and multi-year droughts (Cook et al., 2004; Dai et al., 2004). Identifying the physical conditions in which our ability to estimate ET is most sensitive or limited by knowledge of subsurface geologic properties helps to prioritize regional data acquisition agendas. Integrating results from recent advances in geophysical measurements and models such as those emerging from critical zone observatories in the US and elsewhere (Anderson et al., 2008) will be essential for analysis of climate ET interactions.

*Acknowledgements.* Data are available upon request from the author. This work was supported by funding from the US Geological Survey through the Western Mountain Initiative (award number G09AC00337) and the US National Science Foundation through the Willamette Watershed 2100 project (EAR-1039192). We also acknowledge support from the Southern Sierra Critical Zone Observatory (EAR-0725097) and the Center for Scientific Computing from the CNSI, MRL, an NSF MRSEC (DMR-1121053) and NSF CNS-0960316.

Edited by: P. Saco

## References

- Allen, C. D., Macalady, A. K., Chenchouni, H., Bachelet, D., McDowell, N., Vennetier, M., Kitzberger, T., Rigling, A., Breshears, D. D., Hogg, E. H. (Ted), Gonzalez, P., Fensham, R., Zhang, Z., Castro, J., Demidova, N., Lim, J.-H., Allard, G., Running, S. W., Semerci, A., and Cobb, N.: A global overview of drought and heat-induced tree mortality reveals emerging climate change risks for forests, *For. Ecol. Manage.*, 259, 660–684, doi:10.1016/j.foreco.2009.09.001, 2010.
- Anderson, S. P., Bales, R. C., and Duffy, C. J.: Critical Zone Observatories: Building a network to advance interdisciplinary study of Earth surface processes, *Mineral. Mag.*, 72, 7–10, doi:10.1180/minmag.2008.072.1.7, 2008.
- Arthur, M. and Fahey, T.: Biomass and nutrients in an Engelmann spruce - subalpine fir forest in north central Colorado: pools, annual production, and internal cycling, *Can. J. For. Res.*, 22, 315–325, doi:10.1139/x92-041, 1992.
- Ashfaq, M., Ghosh, S., Kao, S.-C., Bowling, L. C., Mote, P., Touma, D., Rauscher, S. A., and Diffenbaugh, N. S.: Near-term acceleration of hydroclimatic change in the western US, *J. Geophys. Res. Atmos.*, 118, 1–18, doi:10.1002/jgrd.50816, 2013.
- Bales, R., Hopmans, J., O'Green, A., Meadows, M., Hartsough, P., Kirchner, P., Hunsaker, C., and Beaudette, D.: Soil Moisture Response to Snowmelt and Rainfall in a Sierra Nevada Mixed-Conifer Forest, *Vadose Zo. J.*, 10, 786–799, doi:10.2136/vzj2011.0001, 2011.
- Band, L. E., Tague, C. L., Brun, S. E., Tenenbaum, D. E., and Fernandes, R. A.: Modelling Watersheds as Spatial Object Hierarchies: Structure and Dynamics, *Trans. GIS*, 4, 181–196, doi:10.1111/1467-9671.00048, 2000.
- Barnard, H., Graham, C., van Verseveld, W., Brooks, J. R., Bond, B. J., and McDonnell, J. J.: Mechanistic assessment of hillslope transpiration controls of diel subsurface flow: a steady-state irrigation approach, *Ecohydrology*, 3, 133–142, doi:10.1002/eco.114, 2010.
- Baron, J., Hartman, M., and Band, L.: Sensitivity of a high-elevation Rocky Mountain watershed to altered climate and CO<sub>2</sub>, *Water Resour. Res.*, 36, 89–99, 2000.
- Baron, J. S. and Denning, A.: Hydrologic budget estimates, in *Bio-geochemistry of a Subalpine Ecosystem*, edited by: Baron, J., 28–47, Springer-Verlag, New York, 1992.
- Beven, K. J.: *Rainfall-runoff modelling: the primer*, John Wiley & Sons., 119–135, 2011.
- Beven, K. J. and Binley, A.: the future of distributed models: model calibration and uncertainty prediction, *Hydrol. Process.*, 6, 279–298, doi:10.1002/hyp.3360060305, 1992.
- Boisvenue, C. and Running, S. W.: Impacts of climate change on natural forest productivity – evidence since the middle of the 20th century, *Global Change Biol.*, 12, 862–882, doi:10.1111/j.1365-2486.2006.01134.x, 2006.
- Bradford, J. B., Birdsey, R. A., Joyce, L. A., and Ryan, M. G.: Tree age, disturbance history, and carbon stocks and fluxes in subalpine Rocky Mountain forests, *Global Change Biol.*, 14(, 2882–2897, doi:10.1111/j.1365-2486.2008.01686.x, 2008.
- Brooks, P. D., Troch, P. A., Durcik, M., Gallo, E., and Schlegel, M.: Quantifying regional scale ecosystem response to changes in precipitation: Not all rain is created equal, *Water Resour. Res.*, 47, W00J08, doi:10.1029/2010WR009762, 2011.
- Brooks, R. and Corey, A.: Hydraulic properties of porous media, in *Hydrology Paper 3*, p. 27, Colorado State University, Fort Collins, 1964.
- Cayan, D. R., Dettinger, M. D., Kammerdiener, S. A., Caprio, J. M., and Peterson, D. H.: Changes in the Onset of Spring in the Western United States, *B. Am. Meteor. Soc.*, 82, 399–415, doi:10.1175/1520-0477(2001)082<0399:CITOOS>2.3.CO;2, 2001.
- Cook, E. R., Woodhouse, C. A., Eakin, C. M., Meko, D. M., and Stahle, D. W.: Long-term aridity changes in the western United States, *Science*, 306, 1015–1018, doi:10.1126/science.1102586, 2004.
- Dahlgren, R. A., Boettinger, J. L., Huntington, G. L., and Amundson, R. G.: Soil development along an elevational transect in the western Sierra Nevada, California, *Geoderma*, 78, 207–236, doi:10.1016/S0016-7061(97)00034-7, 1997.
- Dai, A., Trenberth, K. E., and Qian, T.: A global dataset of Palmer Drought Severity Index for 1870–2002: Relationship with soil moisture and effects of surface warming, *J. Hydrometeorol.*, 5, 1117–1130, 2004.
- Denning, A., Baron, J., Mast, M., and Arthur, M.: Hydrologic pathways and chemical composition of runoff during snowmelt in Loch Vale watershed, Rocky Mountain National Park, Colorado, USA, *Water. Air. Soil Pollut.*, 59, 107–123, 1991.
- Diffenbaugh, N. S., Scherer, M., and Ashfaq, M.: Response of snow-dependent hydrologic extremes to continued global warming, *Nat. Clim. Chang.*, 3, 379–384, doi:10.1038/nclimate1732, 2013.
- Dingman, S. L.: *Physical Hydrology*, 2nd ed., Prentice Hall, Englewood Cliffs, NJ, p. 236, 1994.
- Famiglietti, J. S., Ryu, D., Berg, A. A., Rodell, M., and Jackson, T. J.: Field observations of soil moisture variability across scales, *Water Resour. Res.*, 44, W01423, doi:10.1029/2006WR005804, 2008.
- Farquhar, G. D., Von Caemmerer, S., and Berry, J. A.: A biochemical model of photosynthetic CO<sub>2</sub> assimilation in leaves of C3 species, *Planta*, 149, 78–90, 1980.
- Flock, J.: Lichen-Bryophyte Distribution along a Snow-Cover-Soil-Moisture Gradient, Niwot Ridge, Colorado, *Arct. Alp. Res.*, 10, 31–47, 1978.
- Garcia, E. S., Tague, C. L., and Choate, J. S.: Method of spatial temperature estimation influences ecohydrologic modeling in the Western Oregon cascades, *Water Resour. Res.*, 49, 1611–1624, doi:10.1002/wrcr.20140, 2013.
- Geroy, I. J., Gribb, M. M., Marshall, H. P., Chandler, D. G., Benner, S. G., and McNamara, J. P.: Aspect influences on soil water retention and storage, *Hydrol. Process.*, 25(, 3836–3842, doi:10.1002/hyp.8281, 2011.
- Gholz, H. L.: Environmental limits on aboveground net primary production, leaf area, and biomass in vegetation zones of the Pacific Northwest, *Ecology*, 63, 469–481, 1982.
- Goulden, M. L., Anderson, R. G., Bales, R. C., Kelly, A. E., Meadows, M., and Winston, G. C.: Evapotranspiration along an elevation gradient in California's Sierra Nevada, *J. Geophys. Res.*, 117, G03028, doi:10.1029/2012JG002027, 2012.
- Grant, G. E., Tague, C. L., and Allen, C. D.: Watering the forest for the trees: an emerging priority for managing water in forest landscapes, *Front. Ecol. Environ.*, 11, 314–321, doi:10.1890/120209, 2013.

- Grier, C. C. and Logan, R. S.: Old-growth *Pseudotsuga menziesii* communities of a western Oregon watershed: biomass distribution and production budgets, *Ecol. Monogr.*, 47, 373–400, 1977.
- Hamlet, A. F., Mote, P. W., Clark, M. P. and Lettenmaier, D. P.: Twentieth-Century Trends in Runoff, Evapotranspiration, and Soil Moisture in the Western United States\*, *J. Clim.*, 20, 1468–1486, doi:10.1175/JCLI4051.1, 2007.
- Hanson, P. and Weltzin, J.: Drought disturbance from climate change: response of United States forests, *Sci. Total Environ.*, 262, 205–220, doi:10.1016/S0048-9697(00)00523-4, 2000.
- Hicke, J. A., Allen, C. D., Desai, A. R., Dietze, M. C., Hall, R. J., Ted Hogg, E. H., Kashian, D. M., Moore, D., Raffa, K. F., Sturrock, R. N., and Vogelmann, J.: Effects of biotic disturbances on forest carbon cycling in the United States and Canada, *Global Change Biol.*, 18, 7–34, doi:10.1111/j.1365-2486.2011.02543.x, 2012.
- Homer, C., Dewitz, J., Fry, J., Coan, M., Hossain, N., Larson, C., Herold, N., Mckerrow, A., Vandriel, J. N., and Wickham, J.: Completion of the 2001 National Land Cover Database for the Conterminous United States, *Photogramm. Eng. Remote Sens.*, 73, 337–341, 2007.
- Hudiburg, T., Law, B., Turner, D. P., Campbell, J., Donato, D., and Duane, M.: Carbon dynamics of Oregon and Northern California forests and potential land-based carbon storage., *Ecol. Appl.*, 19, 163–180, doi:10.1890/07-2006.1, 2009.
- Hwang, T., Band, L., and Hales, T. C.: Ecosystem processes at the watershed scale: Extending optimality theory from plot to catchment, *Water Resour. Res.*, 45, W11425, doi:10.1029/2009WR007775, 2009.
- Isaac, V. and van Wijngaarden, W. A.: Surface Water Vapor Pressure and Temperature Trends in North America during 1948–2010, *J. Clim.*, 25, 3599–3609, doi:10.1175/JCLI-D-11-00003.1, 2012.
- Jarvis, P.: The interpretation of the variations in leaf water potential and stomatal conductance found in canopies in the field, *Philos. Trans. R. Soc. London. B, Biol. Sci.*, 273, 593–610, doi:10.1098/rstb.1976.0035, 1976.
- Kampf, S., Markus, J., Heath, J., and Moore, C.: Snowmelt runoff and soil moisture dynamics on steep subalpine hillslopes, *Hydrol. Process.*, 29, 712–723, doi:10.1002/hyp.10179, 2014.
- Knowles, N., Dettinger, M. D., and Cayan, D. R.: Trends in snowfall versus rainfall in the western United States, *J. Clim.*, 19, 4545–4559, doi:10.1175/JCLI3850.1, 2006.
- Landsberg, J. and Waring, R.: A generalised model of forest productivity using simplified concepts of radiation-use efficiency, carbon balance and partitioning, *For. Ecol. Manage.*, 95, 209–228, 1997.
- Litaor, M. I., Williams, M. and Seastedt, T. R.: Topographic controls on snow distribution, soil moisture, and species diversity of herbaceous alpine vegetation, Niwot Ridge, Colorado, *J. Geophys. Res.*, 113, G02008, doi:10.1029/2007JG000419, 2008.
- Loudermilk, E. L., Scheller, R. M., Weisberg, P. J., Yang, J., Dilts, T. E., Karam, S. L., and Skinner, C.: Carbon dynamics in the future forest: the importance of long-term successional legacy and climate–fire interactions, *Global Change Biol.*, 19, 3502–3515, doi:10.1111/gcb.12310, 2013.
- McGuire, K. J., Weiler, M., and McDonnell, J. J.: Integrating tracer experiments with modeling to assess runoff processes and water transit times, *Adv. Water Resour.*, 30, 824–837, doi:10.1016/j.advwatres.2006.07.004, 2007.
- McNamara, J. P., Chandler, D., Seyfried, M., and Achet, S.: Soil moisture states, lateral flow, and streamflow generation in a semi-arid, snowmelt-driven catchment, *Hydrol. Process.*, 19, 4023–4038, doi:10.1002/hyp.5869, 2005.
- McNamara, J. P., Tetzlaff, D., Bishop, K., Soulsby, C., Seyfried, M., Peters, N. E., Aulenbach, B. T., and Hooper, R.: Storage as a metric of catchment comparison, *Hydrol. Process.*, 25, 3364–3371, doi:10.1002/hyp.8113, 2011.
- Monteith, J.: Evaporation and Environment, in *Proceedings of the 19th Symposium of the Society for Experimental Biology*, Cambridge University Press, New York, 19, 205–234, 1965.
- Moore, I. D., Grayson, R. B., and Ladson, A. R.: Digital terrain modelling?: A review of hydrological, geomorphological, and biological applications, *Hydrol. Process.*, 5, 3–30, 1991.
- Mote, P. W., Hamlet, A. F., Clark, M. P., and Lettenmaier, D. P.: Declining Mountain Snowpack in Western North America\*, *B. Am. Meteor. Soc.*, 86, 39–49, doi:10.1175/BAMS-86-1-39, 2005.
- Muggeo, V. M. R.: Estimating regression models with unknown break-points., *Stat. Med.*, 22, 3055–3071, doi:10.1002/sim.1545, 2003.
- Nash, J. E. and Sutcliffe, J.: River flow forecasting through conceptual models part I – A discussion of principles, *J. Hydrol.*, 10, 282–290, 1970.
- Post, D. A. and Jones, J. A.: Hydrologic regimes of forested, mountainous, headwater basins in New Hampshire, North Carolina, Oregon, and Puerto Rico, *Adv. Water Resour.*, 24, 1195–1210, doi:10.1016/S0309-1708(01)00036-7, 2001.
- Running, S. and Nemani, R.: Extrapolation of synoptic meteorological data in mountainous terrain and its use for simulating forest evapotranspiration and photosynthesis, *Can. J. For. Res.*, 17, 472–483, 1987.
- Ryan, M. G.: Effects of climate change on plant respiration, *Ecol. Appl.*, 1, 157–167, 1991.
- Schwinning, S.: The ecohydrology of roots in rocks, *Ecohydrology*, 3, 238–245, doi:10.1002/eco.134, 2010.
- Shields, C. A. and Tague, C. L.: Assessing the Role of Parameter and Input Uncertainty in Ecohydrologic Modeling: Implications for a Semi-arid and Urbanizing Coastal California Catchment, *Ecosystems*, 15, 775–791, doi:10.1007/s10021-012-9545-z, 2012.
- Smith, T. J., McNamara, J. P., Flores, A. N., Gribb, M. M., Aishlin, P. S., and Benner, S. G.: Small soil storage capacity limits benefit of winter snowpack to upland vegetation, *Hydrol. Process.*, 25, 3858–3865, doi:10.1002/hyp.8340, 2011.
- Sterl, A., Severijns, C., Dijkstra, H., Hazeleger, W., Jan van Oldenborgh, G., van den Broeke, M., Burgers, G., van den Hurk, B., Jan van Leeuwen, P., and van Velthoven, P.: When can we expect extremely high surface temperatures?, *Geophys. Res. Lett.*, 35, L14703, doi:10.1029/2008GL034071, 2008.
- Stewart, I. T., Cayan, D. R., and Dettinger, M. D.: Changes toward Earlier Streamflow Timing across Western North America, *J. Clim.*, 18, 1136–1155, doi:10.1175/JCLI3321.1, 2005.
- Tague, C. and Band, L.: RHESSys: regional hydro-ecologic simulation system-an object-oriented approach to spatially distributed modeling of carbon, water, and nutrient cycling, *Earth Interact.*, 8, 1–42, doi:10.1175/1087-3562(2004)8<1:RRHSSO>2.0.CO;2, 2004.
- Tague, C. and Heyn, K.: Topographic controls on spatial patterns of conifer transpiration and net primary productivity under climate

- warming in mountain ecosystems, *Ecohydrology*, 554, 541–554, doi:10.1002/eco.88, 2009.
- Tague, C. and Peng, H.: The sensitivity of forest water use to the timing of precipitation and snowmelt recharge in the California Sierra: Implications for a warming climate, *J. Geophys. Res. Biogeosci.*, 118, 1–13, doi:10.1002/jgrg.20073, 2013.
- Tang, J., Pilesjö, P., Miller, P. A., Persson, A., Yang, Z., Hanna, E., and Callaghan, T. V.: Incorporating topographic indices into dynamic ecosystem modelling using LPJ-GUESS, *Ecohydrology*, 7, 1147–1162, doi:10.1002/eco.1446, 2013.
- Thompson, S., Harman, C., Konings, A., Sivapalan, M., Neal, A., and Troch, P.: Comparative hydrology across AmeriFlux sites: The variable roles of climate, vegetation, and groundwater, *Water Resour. Res.*, 47, W00J07, doi:10.1029/2010WR009797, 2011.
- Thornton, P. E.: Description of a numerical simulation model for predicting the dynamics of energy, water, carbon, and nitrogen in a terrestrial ecosystem, University of Montana, Missoula, MT, 1998.
- Thornton, P. E. and Rosenbloom, N. A.: Ecosystem model spin-up: Estimating steady state conditions in a coupled terrestrial carbon and nitrogen cycle model, *Ecol. Modell.*, 189, 25–48, doi:10.1016/j.ecolmodel.2005.04.008, 2005.
- Thornton, P., Thornton, M., Mayer, B., Wilhelmi, N., Wei, Y., and Cook, R.: Daymet: Daily surface weather on a 1 km grid for North America, 1980–2012, Oak Ridge Natl. Lab. Distrib. Act. Arch. Cent., doi:10.3334/ORNLDAAAC/Daymet\_V2, 2012.
- Trujillo, E., Molotch, N. P., Goulden, M. L., Kelly, A. E., and Bales, R. C.: Elevation-dependent influence of snow accumulation on forest greening, *Nat. Geosci.*, 5, 705–709, doi:10.1038/ngeo1571, 2012.
- van Mantgem, P. J., Stephenson, N. L., Byrne, J. C., Daniels, L. D., Franklin, J. F., Fulé, P. Z., Harmon, M. E., Larson, A. J., Smith, J. M., Taylor, A. H., and Veblen, T. T.: Widespread increase of tree mortality rates in the western United States, *Science*, 323, 521–524, doi:10.1126/science.1165000, 2009.
- Vicente-Serrano, S. M., Camarero, J. J., Zabalza, J., Sangüesa-Barreda, G., López-Moreno, J. I., and Tague, C. L.: Evapotranspiration deficit controls net primary production and growth of silver fir: Implications for Circum-Mediterranean forests under forecasted warmer and drier conditions, *Agr. For. Meteorol.*, 206, 45–54, doi:10.1016/j.agrformet.2015.02.017, 2015.
- Webb, W., Szarek, S., Lauenroth, W., Kinerson, R., and Smith, M.: Primary Productivity and Water Use in Native Forest, Grassland, and Desert Ecosystems, *Ecology*, 59, 1239–1247, doi:10.2307/1938237, 1978.
- Williams, A., Allen, C., Macalady, A., Griffin, D., Woodhouse, C., Meko, D., Swetnam, T. W., Rauscher, S. A., and Seager, R.: Temperature as a potent driver of regional forest drought stress and tree mortality, *Nat. Clim. Chang.*, 3(September), 292–297, doi:10.1038/NCLIMATE1693, 2013.
- Zierl, B., Bugmann, H., and Tague, C.: Water and carbon fluxes of European ecosystems: An evaluation of the ecohydrological model RHESSys, *Hydrol. Process.*, 21, 3328–3339, doi:10.1002/hyp.6540, 2007.